Improvement of Vibration Suppression Performance of Galvano Mirror Using Piezoelectric Element

Kenta Seki, Hiroki Yokoi and Makoto Iwasaki
Department of Computer Science & Engineering
Nagoya Institute of Technology
Nagoya, Japan
Email: k-seki@nitech.ac.jp

***Abstract*— This paper presents a vibration suppression approach for galvano mirrors in laser positioning systems. The systems require the fast and high-precision positioning of the mirror and should maintain the flatness of the mirror after positioning to ensure the control performance. However, resonant vibrations of the mirror, which are excited by the moment force during positioning, lead to residual vibrations after positioning, deteriorating the flatness of the mirror and laser manufacturing accuracy. In this paper, therefore, a vibration suppression approach is proposed by mounting a piezoelectric element on the mirror, where a multi-function of the piezoelectric element as an actuator and a sensor are applied to design the vibration suppression controller. The applicability of the proposed approach to industrial galvano scanners has been verified by performing experiments using a prototype.**

I. Introduction

Laser-drilling machine [1] [2] is one of typical machine tools for electronics manufacturing, that is scanning laser beams to arbitrary positions by galvano scanners, and drill via holes on printed wired boards (PWBs). The galvano scanner [3] is composed of a servo motor and a galvano mirror to reflect the laser beam. That is, the fast and high precision positioning of galvano scanner should be a key technique to achieve higher productivities of laser-drilling machines. In order to provide the requirements, a variety of control approaches have been proposed and implemented to the actual systems [4] [5]. Among them, although the mirror is indirectly controlled by an angular sensor on the motor shaft as a semi-closed control system, behaviors of the mirror and/or irradiated position of laser beam on the PWBs cannot be directly evaluated and controlled. The mirror is a flat plate whose mechanical structure is a cantilever beam supported on the motor shaft edge. Therefore, the mirror is essentially distorted by a force of moment during positioning, resulting in the vibration of mirror according to its vibration modes. As a result, the drilling accuracy of a via hole is deteriorated as the laser irradiation position shifts.

In this paper, a piezoelectric element (PZT: lead zirconate titanate) is directly mounted on the mirror to improve the vibratory behaviors of the mirror [6]. Since the PZT has a multi-function of both sensor and actuator, detection and suppression of mechanical vibrations can be simultaneously achieved by one element (called SSA: self-sensing actuation) [7]. In the SSA, control states in the signal are generally separated by using an electrical bridge circuit, where a virtual bridge circuit [8] can be applied to reduce the analog devices, e.g. capacitor and resistor, considering an easy tuning of the bridge balance. In order to improve the vibration suppression performance of the mirror, a feedforward compensation signal is generated on the basis of the mathematical model to cancel the vibration source. In addition, a feedback compensator based on the detected signal through the bridge circuit can be designed to reduce effects of modeling errors in the feedforward compensator and parameter variations of the plant. Effectiveness of the proposed approach has been verified by experiments using a prototype of galvano scanners.

II. Positioning Mechanism and Positioning Control System

A. Configuration of positioning mechanism

Fig. 1 shows a configuration of positioning device for the galvano scanner as an experimental setup. The galvano scanner is composed of a servo motor with a mirror, where the motor angle y_s is detected by a sensor and is transferred in a digital signal processor (DSP) controller through an interface with the sampling period of $20\mu s$. The servo motor is driven by a current controlled amplifier with the control input u generated by the position controller. A PZT, on the other hand, is mounted on the mirror to detect and suppress the bending vibration mode, where a bridge circuit is applied to separate the sensor signal v_s and actuator signal v_c from output voltage v_p and input voltage v_a of the PZT. The control signal of PZT u_p is calculated by the DSP. Since the laser irradiation position cannot be directly detected by the motor angle sensor, the direction of two dimensions, i.e. rotational y_r and vertical y_v, is measured and evaluated by a position sensitive detector (PSD) using a semiconductor laser for detection use [4] [6].

B. Plant characteristics

The galvano scanner can be modeled by a multi-degrees of freedom vibration system whose frequency characteristic of y_s for u is plotted by solid lines in Fig. 2, while a frequency characteristic of y_r for u is plotted by solid lines in Fig. 3. From these figures, the mechanism includes the primary vibration mode (1300 Hz), the 2nd vibration mode (4400

978-1-4673-2421-2/12/$31.00 ©2012 IEEE

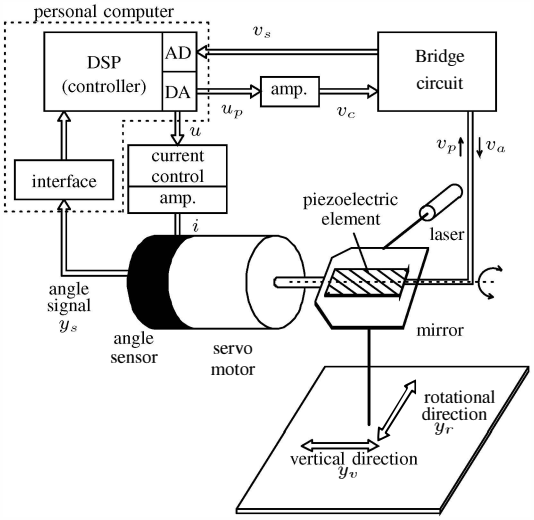

Fig. 1. Configuration of experimental setup with PZT as SSA system.

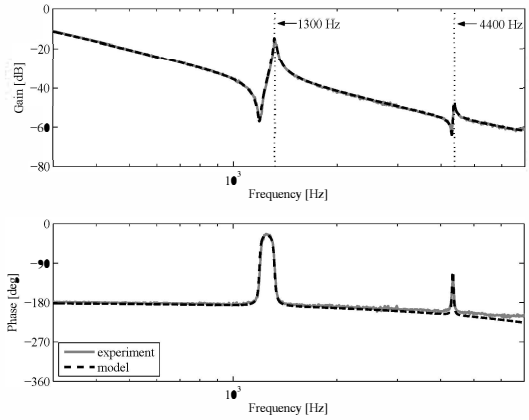

Fig. 2. Frequency characteristics of motor angle y_s for control input u.

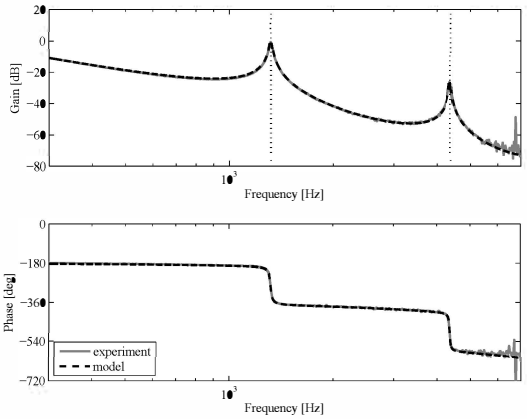

Fig. 3. Frequency characteristics of rotational direction displacement y_r for control input u.

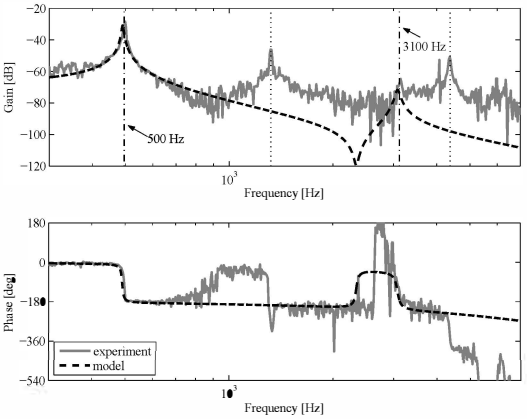

Fig. 4. Frequency characteristics of vertical direction displacement y_v for control input u.

Hz), and a dead time component due to the delay in current controller. These vibration modes are caused by twist of shaft [5]. By considering two vibration modes, the following non-parametric models can be formulated as plant mathematical models P_s and P_r, consisting of a rigid mode, vibration modes up to $n = 2$, and a dead time component:

$$P_s = \frac{y_s}{u} = \frac{K_p}{J}\left(\frac{1}{s^2} + \sum_{n=1}^{2} \frac{k_{sn}}{s^2 + 2\zeta_{sn}\omega_{sn}s + \omega_{sn}^2}\right) e^{-Ls}, \quad (1)$$

$$P_r = \frac{y_r}{u} = \frac{K_p}{J}\left(\frac{1}{s^2} + \sum_{n=1}^{2} \frac{k_{rn}}{s^2 + 2\zeta_{sn}\omega_{sn}s + \omega_{sn}^2}\right) e^{-Ls}, \quad (2)$$

where K_p: gain which includes torque constant of motor, and current control gain, J: moment of inertia, ω_{sn}: natural angular frequency of nth vibration mode, ζ_{sn}: damping coefficient of nth vibration mode, k_{sn} and k_{rn}: modal constants of nth vibration mode, and L: equivalent dead time, respectively. The broken lines in Figs. 2 and 3 show the frequency characteristics of the mathematical models P_s and P_r.

Solid lines of Fig. 4, on the other hand, shows a frequency characteristic of y_v for u. From the Fig. 4, other vibration modes shown in vertical chain lines exist at 500 and 3100 Hz. Although the twist vibration modes can not be detected in the vertical direction, bending of the mirror caused by twist vibrations is detected as the vertical displacement in this measurement system. These vibration modes in 500 and 3100 Hz are generated as bending modes which are caused by the support of the fixed end of the mirror as the fulcrum shown in the FEM analysis results in Fig. 5.

C. Positioning control system

Since the galvano scanner positioning system cannot generally detect the laser irradiation position as explained in Fig. 1, a semi-closed control system using motor angle y_s should be constructed. Fig. 6 shows a block diagram of an actual 2-degrees-of-freedom positioning system based on

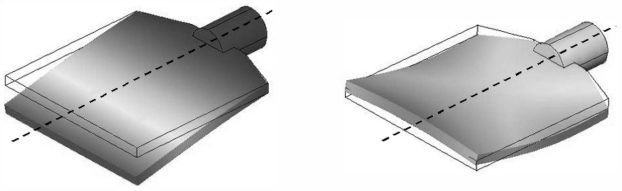

(a) 500 Hz (b) 3100 Hz

Fig. 5. Mode shapes of mirror by FEM analyses.

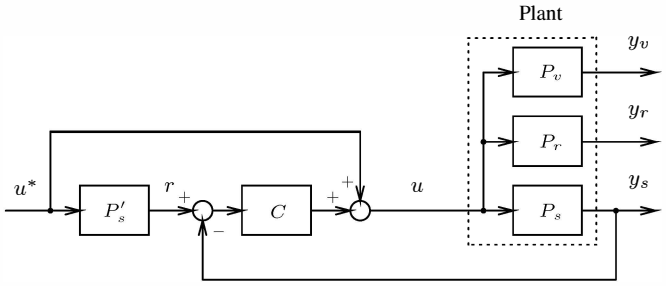

Fig. 6. Block diagram of 2DOF positioning system.

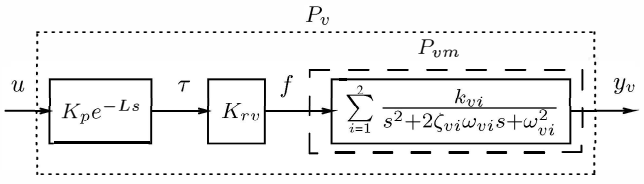

Fig. 7. Block diagram of bending vibration model.

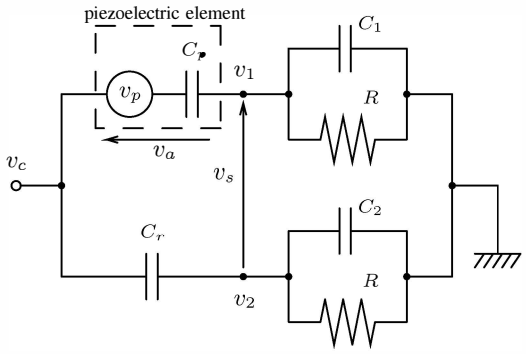

Fig. 8. CC bridge circuit for isolation of signals in PZT voltage.

the final-state control (FSC) [9], where P_s denotes plant system of y_s for u, P_r and P_v denote plant systems of laser irradiation positions (mirror rotational and vertical direction displacements y_r and y_v shown in Fig. 1) for u, C denotes position feedback compensator including phase lead-lag filter and notch filters, P_s' denotes a nominal transfer function for P_s including the 1st and 2nd twist vibration modes (1300 and 4400 Hz), r is motor angle reference corresponding to laser irradiation position (rotational direction displacement y_r), u^* is feedforward control input based on the FSC.

The desired control specification for the positioning system is given that a point-to-point positioning for the typical stroke (laser irradiation position) of 1.5 mm should be settled within 2.0 ms.

III. Modeling of Bending Vibration Modes and Signal Isolation in SSA

A. Modeling of bending vibration modes

Since the motor torque generates only in the rotational direction of the galvano scanner, excitation of bending vibration modes in Fig. 4 cannot be observed. However, force of the vertical direction against the mirror surface caused by rotational unbalance generates and excites the bending vibration modes. By defining a coefficient K_{rv} from torque τ to excitation force f of bending direction, a mathematical model P_v for the bending vibration modes can be expressed by:

$$P_v = \frac{y_v}{u} = K_p K_{rv} \left(\sum_{n=1}^{2} \frac{k_{vn}}{s^2 + 2\zeta_{vn}\omega_{vn}s + \omega_{vn}^2} \right) e^{-Ls}, \tag{3}$$

where, K_p and L are the same parameters as in (1), ω_{vn}: natural angular frequency of nth bending vibration mode, ζ_{vn}: damping coefficient of nth bending vibration mode, and k_{vn}: modal constant of nth bending vibration mode, respectively. Broken lines in Fig. 4 show a frequency characteristic of the mathematical model P_v. Block diagram of this bending vibration modes, therefore, can be expressed as shown in Fig. 7. In the figure, τ is actual motor torque.

It is essentially difficult to remove the mechanical rotational unbalance. In addition, since the primary bending vibration mode (500 Hz) is lower than the primary twist vibration mode (1300 Hz) and it exists within the servo bandwidth, the bending vibration mode can be easily excited.

B. Signal isolation by bridge circuit

In this research, a PZT is directly mounted on the mirror along the rotational axis as shown in a dotted line of Fig. 5 to effectively detect and suppress the bending vibration modes, where a SSA simultaneously plays the roles of both sensor and actuator. In the SSA, since the PZT is applied as both a sensor and an actuator, the voltage of the PZT includes both sensing and actuating states. As indicated in Fig. 1, therefore, the voltage should be isolated by a bridge circuit [7]. Fig. 8 shows a CC bridge circuit to isolate the signals in the voltage. In the figure, the PZT can be expressed by an output voltage v_p caused by deformation of mirror and an equivalent capacitance C_p, while v_c denotes supplied voltage to bridge circuit, v_s denotes sensor voltage, v_a denotes input voltage to the PZT (actuation voltage), C_r, C_1, C_2 denote capacitances, and R denotes resistance to remove the offset of signal. From the figure, voltage equations of the bridge circuit are given as follows.

$$v_1 = \frac{C_p R s}{1 + (C_p + C_1)Rs} \{v_c + v_p\} \tag{4}$$

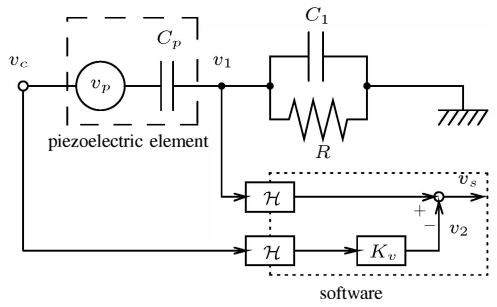

Fig. 9. Virtual CC bridge circuit for isolation of signals in voltage.

$$v_2 = \frac{C_r Rs}{1+(C_r+C_2)Rs} v_c \tag{5}$$

In order to satisfy the well-known bridge balance of $C_p = C_r$ and $C_1 = C_2$, the following equations can be derived.

$$v_s = v_1 - v_2 = \frac{C_p Rs}{1+(C_p+C_1)Rs} v_p \tag{6}$$

$$v_a = v_c - v_1 = \frac{C_1}{C_p+C_1} v_c \tag{7}$$

From (6), the output voltage v_p can be extracted by the potential difference between v_1 and v_2. Here, since angular frequency ω_b of the bridge circuit is set to $\omega_b \gg \frac{1}{(C_p+C_1)R}$ by R, (6) can be expressed by:

$$v_s \simeq \frac{C_p}{C_p+C_1} v_p. \tag{8}$$

From (8), the sensor voltage v_s is proportional to the output voltage v_p. From (7), on the other hand, the supplied voltage to bridge circuit v_c is proportional to the actuation voltage v_a. However, it is actually difficult to satisfy the bridge balance of $C_p = C_r$ and $C_1 = C_2$. Especially, C_r completely corresponding to the value of C_p cannot be always implemented by a circuit element.

In order to solve the problem, a part of CC bridge circuit in Fig. 8 can be constructed by a software as a virtual bridge circuit [8]. From (5), since v_2 is determined by supplied voltage v_c regardless of v_p, v_2 may not need to be directly measured by the analog circuit. Therefore, Fig. 8 can be modified as Fig. 9 by constructing the lower part of the circuit as the software. In the Fig. 9, $\mathcal{H}$ denotes a holder by an A/D converter, and K_v can be given as follows based on (5).

$$K_v = \frac{C_r Rs}{1+(C_r+C_2)Rs} \tag{9}$$

As a result, the sensor voltage v_s in (6) can be easily calculated only by R and C_1 as the circuit elements.

IV. Controller Design

By using the bending vibration mode model P_{vm}, (7), and (8) acquired through the balanced bridge circuit, a positioning control system with SSA control system can be designed as a block diagram in Fig. 10, where K_ϕ: coefficient of transformation from mechanical energy to electrical energy,

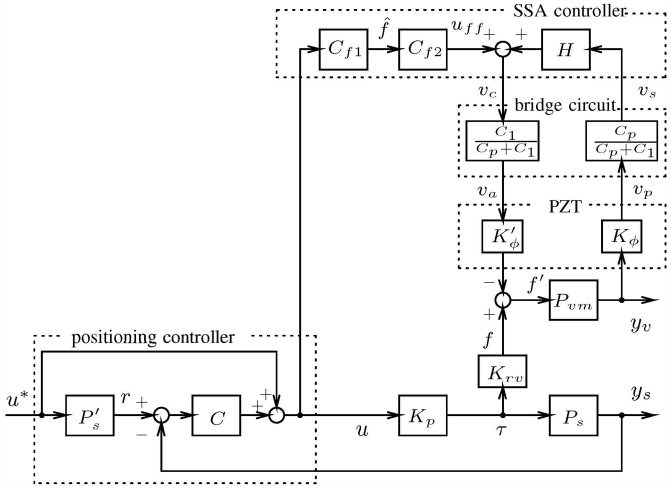

Fig. 10. Block diagram of positioning system with SSA system.

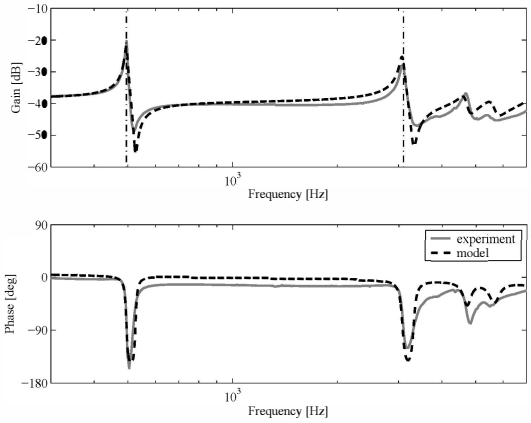

Fig. 11. Frequency characteristics of sensor voltage v_s for supplied voltage v_c.

K'_ϕ: coefficient of transformation from electrical energy to mechanical energy, H: feedback compensator of SSA control system, C_{f1} and C_{f2}: feedforward compensators, $\hat{f}$: estimated f, and u_{ff}: feedforward signal, respectively. In the SSA control system, since the mirror bends by the force of vertical direction f, the vertical displacement y_v occurs. Then, the output voltage v_p is generated by a piezoelectric effect of the PZT, while the sensor voltage v_s is detected by the bridge circuit. By supplying the voltage v_c through the compensators C_{f1}, C_{f2}, and H to the bridge circuit, the actuation voltage v_a is given to the PZT. As a result, the excitation force by the inverse piezoelectric effect can suppress the bending vibration of mirror.

Fig. 11 indicates frequency characteristics of sensor voltage v_s for supplied voltage v_c to the virtual CC bridge circuit in Fig. 9. In the figure, solid lines indicate results in experiment, while broken lines indicate ones of simulation model. From the figure, both sensing and actuating of the bending vibration modes can be isolated by the bridge circuit. The feedback

compensator H, therefore, can be designed on the basis of the characteristics in Fig. 11.

In this research, a feedforward signal u_{ff} is calculated to cancel the force of vertical direction f by mathematical model, where dead time component L can be ignored within the control bandwidth. From the block diagram of Fig. 10, C_{f1} and C_{f2} are designed as follows:

$$C_{f1} = K_p K_{rv}, \tag{10}$$

$$C_{f2} = \frac{1}{K'_\phi \frac{C_1}{C_r+C_1}}. \tag{11}$$

The feedback compensator H, on the other hand, can be designed to suppress the effect of modeling errors and parameter variations in (10) and (11). From Fig. 10, a sensitivity function f'/f can be calculated as follows.

$$\frac{f'}{f} = \frac{1}{1 + P_{vm} \cdot \frac{K_\phi C_r}{C_r+C_1} \cdot \frac{K'_\phi C_1}{C_r+C_1} \cdot H} = \frac{1}{1+G_o} \tag{12}$$

Here, G_o is an open-loop transfer function of the SSA feedback loop. From (12), the sensitivity function f'/f can be shaped by the open-loop transfer function G_o, which can be arbitrarily shaped by the feedback compensator H.

As a relationship between open-loop transfer function and sensitivity function, it is known that the sensitivity of control system decreases by receding the vector locus of the open-loop transfer function in the complex plane from the critical point of $(-1, j0)$ [10]. Therefore, the vector locus of the primary bending vibration mode should be considered to draw a larger mode circle greatly in the right side in the complex plane. In addition, in order to avoid the spillover of higher vibration modes, the feedback gains should be decreased in the high frequency range. The compensator H, therefore, can be designed as the following bandpass filter:

$$H = K_c \frac{s^2}{s^2 + 2\zeta_{c1}\omega_{c1}s + \omega_{c1}^2} \frac{\omega_{c2}^2}{s^2 + 2\zeta_{c2}\omega_{c2}s + \omega_{c2}^2}, \tag{13}$$

where K_c =40, $\omega_{c1} = 2\pi \times 100$ rad/s, $\omega_{c2} = 2\pi \times 500$ rad/s, $\zeta_{c1} = 0.7$, and $\zeta_{c2} = 0.7$. Fig. 12 indicates a Nyquist diagram of the SSA control system with the designed compensator H, where a black solid line represents the nominal condition without parameter variation, blue dotted and broken lines represent the cases with ± 5 % variation in capacitance C_r, and red dotted and broken lines represent the cases with ± 5 % variation in capacitance C_2, respectively. In the variations, bridge unbalance is simulated by changing the parameters of virtual bridge circuit. Fig. 13, on the other hand, indicates the sensitivity gain at around the primary bending vibration mode frequency. From Fig. 12, the desired vector loci due to the primary bending vibration mode can be drawn in the right side in the complex plane. As a result, the gain can be reduced in the primary bending vibration mode as shown in the sensitivity gain of Fig.13. In addition, the SSA system is stable under the ± 5 % variations of capacitance.

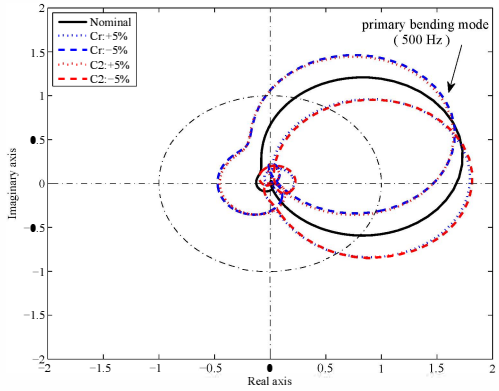

Fig. 12. Nyquist diagrams of SSA control system.

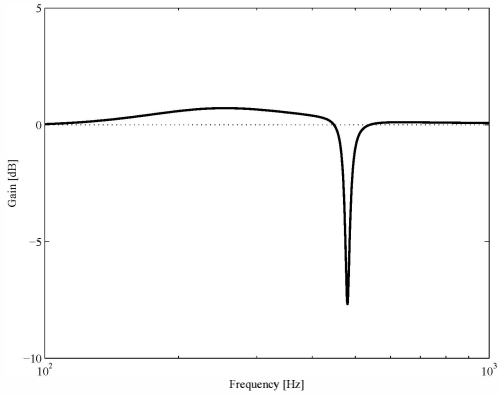

Fig. 13. Sensitivity gain of SSA system (f'/f).

V. Experimental Verifications

The proposed approach has been verified by experiments using the galvano scanner shown in Fig. 1, where the 2DOF positioning control framework has been applied with the proposed SSA system as in Fig. 10. The compensators are implemented as discrete transfer functions by a bilinear transformation with the sampling time 20 μs. Fig. 14 shows experimental results for the target position of 1.5 mm, where the upper waveforms are positioning errors of laser irradiation position (rotation) y_r, and the bottom waveforms are the vertical direction displacements y_v. In the figure, the black lines represent responses without SSA, the blue lines represent ones with SSA feedback compensator H, the green lines represent ones with feedforward compensators, and the red lines represent ones with SSA feedback compensator and feedforward compensators. From Fig. 14, the waveforms of rotational direction displacement show the same performance in both with and without SSA system. Although the bending vibration can be attenuated by applying SSA as indicated in the bottom of Fig. 14, the performance of vibration suppression is insufficient concerning the settling time. In addition, the residual vibration occurs after the settling in the feedfor-

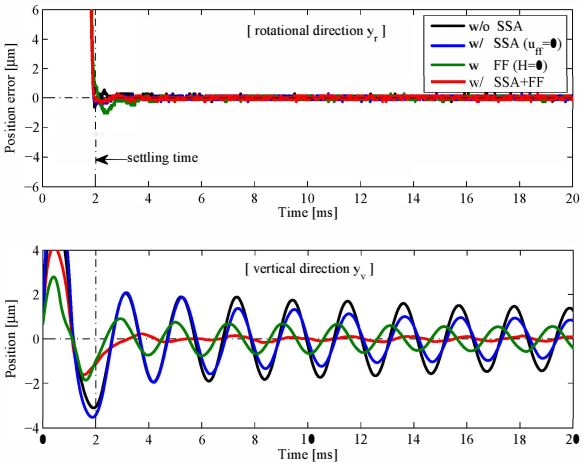

Fig. 14. Experimental waveforms of positioning.

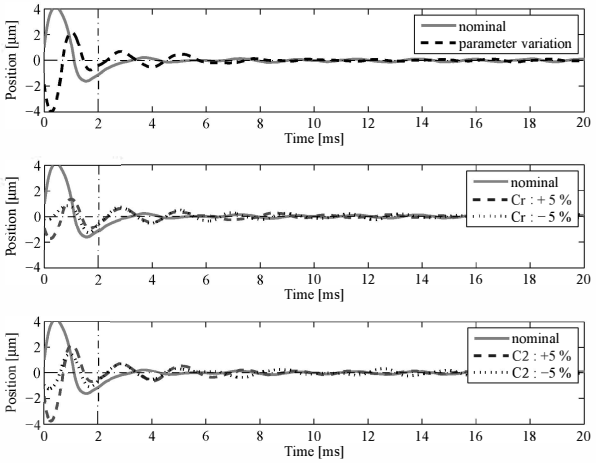

Fig. 15. Experimental waveforms of positioning error with parameter variation.

ward compensation without SSA feedback compensator due to the modeling errors between the compensators and the actual parameters ($K_p, K_{rv}, K'_\phi, C_p, C_1$). On the other hand, the bending vibration after positioning can be completely suppressed by applying the feedforward compensators and the SSA feedback compensator.

Fig. 15 shows experimental results in the cases with the parameter variations, where the waveforms of vertical direction displacement are indicated. Top figure shows waveforms under the parameter variation, where the gain of feedforward compensators is set with 10 % variation. Middle and bottom figures show the waveforms under the bridge unbalance, where C_r and C_2 are changed $\pm$ 5 % by software. From these results, sufficient suppression performance of bending vibration can be achieved under the conditions. However, since the SSA system becomes unstable under the capacitance variation over 10 %, a parameter identification approach in online manner should be developed to apply the advantage of virtual bridge circuit as the future works.

VI. Conclusions

This paper presented a vibration suppression approach of the galvano mirror, where the SSA using PZT was applied to improve the bending vibration suppression performance. The residual vibration of the laser irradiation position excited during positioning was caused by bending vibration of the mirror. In order to suppress the mirror vibration, a PZT was directly mounted on the mirror. The signals of both sensor and actuator included in the voltage of the PZT were isolated by the virtual CC bridge circuit. Then, the SSA control system was constructed. In order to sufficiently suppress the vibration, feedforward compensators were designed on the basis of the mathematical model. The feedback compensator of SSA system, on the other hand, was designed paying attention to the relationship between the sensitivity function and the open-loop transfer function to reduce the sensitivity gain at around the primary bending vibration frequency. The effectiveness of the proposed approach has been verified by experiments using the prototype.

References

[1] R. S. Patel, T. F. Redmond, C. Tessler, D. Tudryn and D. Pulaski, "Via production benefits from excimer-laser tools", *Laser Focus World*, Vol.32, No.1, pp.71–75, 1996.

[2] M. F. Chen and Y. P. Chen, "Compensating technique of field-distorting error for the CO_2 laser galvanometric scanning drilling machines", *Int. Journal of Machine Tools & Manufacture*, Vol.47, No.7-8, pp.1114–1124, 2007.

[3] M. Nirei, Y. Yamamoto, K. Kobayashi and T. Maruyama, "Torque Form Design of Laser Scanning Actuator Based on Statistical Method", *IEEE Trans. on Magnetics*, Vol.33, No.5, pp.4242–4244, 1997.

[4] N. Hirose, M. Iwasaki, M. Kawafuku and H. Hirai, "Initial Value Compensation Using Additional Input for Semi-Closed Control Systems", *IEEE Trans. on Industrial Electronics*, Vol.56, No.3, pp.635–641, 2009.

[5] K. Seki, K. Mochizuki, M. Iwasaki and H. Hirai: "High-Precision Positioning Considering Suppression of Resonant Vibration Modes by Strain Feedback", *Proc. of the 35th Annual Conference of the IEEE Industrial Electronics Society*, pp.3114–3119, 2009.

[6] K. Seki, H. Kannami, M. Iwasaki and H. Hirai, "Application of Self-Sensing Actuation Using Piezoelectric Element for Vibration Suppression of Galvanometric Mirror", *Proc. of 2010 IEEE/ASME International Conference on Advanced Intelligent Mechatronics*, pp.673–678, 2010.

[7] J.J. Dosch, D.J. Inman and E. Garcia: "A Self-Sensing Piezoelectric Actuator for Colocated Control", *J. Intelligent Material Systems and Structures*, Vol.3, pp.166–185, 1992.

[8] T. Takigami, K. Oshima, Y. Hayakawa and M. Ito, "Application of self-sensing actuator to control of a soft-handling gripper", *Proc. of 1998 IEEE International Conference on Control Application*, pp.902–906, 1998.

[9] M. Hirata, T. Hasegawa and K. Nonami, "Seek Control of Hard Disk Drives Based on Final-State Control Taking Account of the Frequency Components and the Magnitude of Control Input", *Proc. of 7th International Workshop on Advanced Motion Control*, pp.40–45, 2002.

[10] T. Atsumi, A. Okuyama and M. Kobayashi, "Track-Following Control Using Resonant Filter in Hard Disk Drives", *IEEE/ASME Trans. on Mechatronics*, Vol.12, No.4, pp.472–479, 2007.